






## Influence of the pressure on the interaction between stearic acid and Ar-O<sub>2</sub> in inductively coupled radio frequency plasma

Euclides Alexandre Bernardelli<sup>1</sup> , Fernanda Splett<sup>1</sup> , Carlos Eduardo Farias<sup>1</sup> ,  
Rodrigo Lupinacci Villanova<sup>2</sup> , Márcio Mafra<sup>1</sup> 

<sup>1</sup>Universidade Tecnológica Federal do Paraná, Departamento Acadêmico de Mecânica. Curitiba, PR, Brasil.

<sup>2</sup>Universidade Tecnológica Federal do Paraná. Curitiba, PR, Brasil.

e-mail: mafra@utfpr.edu.br, ebernardelli@utfpr.edu.br, fernanda.splett@gmail.com, carlos.ed.farias@hotmail.com, villanova@utfpr.edu.br

### ABSTRACT

This work aimed to analyze the influence of treatment pressure on the interaction between stearic acid and an Argon-Oxygen plasma. The fixed variables were the applied RF plasma power (50 W), treatment time (30 min), and treatment starting temperature (273 K). The pressure was varied as follows: 0.2, 0.6, and 1.0 Torr. For all treatment conditions, the etching of the samples was observed, as evidenced by the mass loss of the specimens and by following the gaseous by-products of reactions employing a mass spectrometer coupled to the reaction chamber. Optical emission spectroscopy followed the emission lines of oxygen active species. Functionalization of the specimens was also observed, as shown by the results obtained by Fourier-transform infrared spectroscopy (FTIR) and through XRD analysis. A liquid phase was formed for samples treated at 0.6 and 1.0 Torr, which favored the functionalization process and broadened the band present in the region from 1750 to 1700 cm<sup>-1</sup>, resulting in amorphous phases. An increase in the intensity of the characteristic peaks of esters was also observed. It can be concluded that the higher pressure favors the formation of a liquid phase and reaction kinetics, resulting in higher functionalization and lower etching.

**Keywords:** Plasma Cleaning; Stearic Acid; Pressure; Degradation.

### 1. INTRODUCTION

Metal parts submitted to surface treatments, such as nitriding, galvanizing, and painting, are usually contaminated with oils, grease, and cutting fluids from the manufacturing process. This contamination can hinder the efficiency of surface treatments. Even on a laboratory scale, the cleanness of the surface is mandatory to achieve the best thermochemical treatment performance [1]. During the cleaning processes, non-biodegradable or even toxic compounds are used, which can be harmful to the environment. Hence, there is an important need for environmentally friendly cleaning processes. Besides well-studied processes such as plasma nitriding [2], nitrocarburizing [3], and plasma electrolytic oxidation [4], plasma technology has also been studied for cleaning purposes and has shown great potential for development.

Some authors worked with oil removal from metal surfaces using plasma [5–8], and other authors [9, 10] showed the importance of plasma cleaning in some industry fields, especially aeronautics. The study of the degradation kinetics of organic compounds has received attention given the complexity of reaction paths that can be followed and their influence on the characteristics of the degraded material, either for its use [11] or removal [7, 12–14]. The species in the plasma interact chemically and physically with the compounds on the surface [15, 16], degrading them and forming volatile compounds that are removed from the vacuum system [10].

In order to understand the interaction mechanisms between plasma and organic compounds, the reaction pathways for degradation are studied using plasma and molecular compounds with a simple and known chemical structure [12]. Molecules widely used as models for surface contaminants are stearic acid and hexatriacontane. Works carried out with these compounds [12–14, 17–22] evaluated the influence of the types of discharge and process parameters such as gas composition, pressure, power, and frequency of the electrical source.

Results obtained by those works show the formation of new structures by functionalization or branching of the carbon chains, describing the reaction pathways of etching and transformation. It should be noted that the focus of those studies was the modification of the substrate materials. However, describing the type of volatile

compounds formed during plasma cleaning and their amounts is very important in developing the process. The macroscopic parameters of the discharge also need to be considered, as these directly influence the plasma reactivity [23].

Thus, this work aims to evaluate how the pressure in an ICP radiofrequency plasma influences the degradation process of stearic acid, determining the types and amounts of volatile compounds formed during the process.

## 2. MATERIALS AND METHODS

Stearic acid (SA) is an organic compound with a linear chain of 18 carbon atoms and an acidic functional group at one end ( $C_{18}H_{36}O_2$ ). This compound (Sigma-Aldrich®, 95% pure) was melted, poured, and solidified in a pre-heated specimen holder made of PTFE. The specimen holder was pre-heated in order to slow down the solidification rate, thus increasing the crystallinity of the specimens. The specimen holder is shown in Figure 1. The samples were poured directly on the sample holder, with an exposition surface of  $18 \times 23$  mm. The mass of each specimen was measured with an analytical balance Shimadzu® model AUV220D (resolution of 0.01 mg) before and after the plasma treatment to determine the mass loss.

The reactor shown in Figure 1 is composed of a borosilicate glass tube with an internal diameter of 34 mm and length of 650 mm. The tube is fixed by two brass supports connected to inlet and outlet gas valves, a pressure regulator valve, and an Agilent Technologies® model IDP-15 Dry Scroll Vacuum Pump, which is connected to the reactor outlet. Plasma is produced by means of a copper coil with nine turns connected to a Tokyo Hi-Power® 13,56 MHz radiofrequency source. In order to protect the measuring devices, Faraday cages were used to involve the flow meters and the reactor. The pressure was controlled using Pirani pressure gauges and the valve located at the reactor outlet.

The temperature of the treatments was controlled with the aid of a cooling system containing water and ice in equilibrium. This system comprises a thermal reservoir, a water pump, and a thermal insulator made of acrylic lined with polystyrene, which involves the reactor glass tube. Temperature is monitored with a type K thermocouple placed in a small hole in the specimen holder, just below the area where the material was poured and solidified. After treatments, the specimens were weighted. The temperature and mass loss graphs were plotted with error bars referring to the combined uncertainties of the measuring instruments and material variability with a 95% confidence interval. Four repetitions of treatments were conducted for each pressure value (0.2, 0.6 and 1.0 Torr). The fixed experimental conditions were Plasma Power (50W), Treatment Time (30 min), Gas mixture (90% Ar + 10% Oxygen) and Gas flow (50 SCCM).

After plasma treatments, specimens were characterized employing Fourier-transform infrared spectroscopy (FTIR) and X-ray diffraction (DRX). A Shimadzu® XDR-7000 X-Ray Diffractometer was used, with the following parameters: Cu 11.16 target, current of 30 A, tension of 40 V, scanning rate of  $1^\circ/\text{min}$ , scanning ranges from  $5^\circ$  to  $60^\circ$ , continuous scanning mode, and incidence angle of  $3^\circ$ . A Varian® 640 – FT-IR with ATR and resolution of  $4 \text{ cm}^{-1}$  was used for the FTIR analyses.

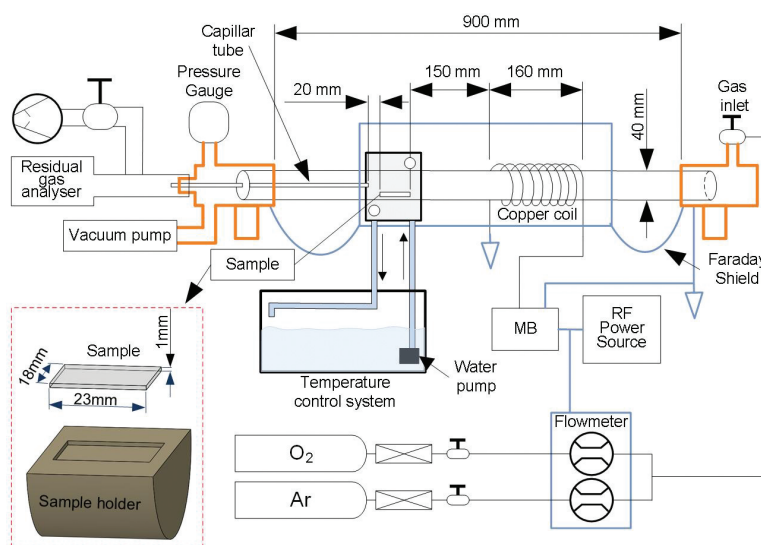


**Figure 1:** Experimental device used to conduct the experiments. Detail: specimen holder.

Plasma analyses were made through optical spectroscopy. A Horiba iHR550 Imaging Spectrometer with a resolution of 0.55 nm was used for that purpose. Treatments with mass spectroscopy were also conducted with a Residual Gas Analyser ACCU QUAD™ from Kurt J. Lesker Company.

### 3. RESULTS AND DISCUSSION

The visual aspect of the specimens treated with different pressures, as well as non-treated samples, is shown in Figure 2. No changes in the visual aspect for specimens treated at 0.2 Torr were observed. For specimens treated with pressures of 0.6 and 1.0 Torr, melted regions of the specimen surfaces can be observed, with larger melted areas when stearic acid was treated with 1.0 Torr.

The average specimen temperature curves are shown in Figure 3. The temperatures are very close for pressures of 0.6 and 1.0 Torr, while the temperature is lower in the treatments at 0.2 Torr. The heat generated by collisions and exothermal reactions at pressures of 0.6 and 1.0 Torr was enough to partially melt the surface of the specimens, which was not observed for treatments at 0.2 Torr pressure (Figure 3). It must be noted that for all treatment conditions, the temperature did not reach 343 K, which is the melting temperature of stearic acid, proving that the formation of the liquid phase is due to the degradation of the stearic acid, leading to the formation of compounds with lower melting points [19, 20].

As can be observed from Figure 4, the increase in treatment pressure causes an increase on the intensity of the peaks related to atomic oxygen species (777.16, 777.39, 777.51, and 884.53 nm) [24]. Such oxygen species increase favors stearic acid's degradation by removing hydrogen from the carbon chain and forming an alkoxy radical [25, 26].

Molecular oxygen (excited or non-excited) present in the plasma also contributes to the degradation process of stearic acid. Some authors proposed the following reaction pathway [18, 25, 26]: formation of a peroxide radical, which reacts with another molecule of stearic acid to form a hydroperoxide, releasing an OH group with subsequent β-split and formation of volatile compounds, as illustrated in Eq. 1.

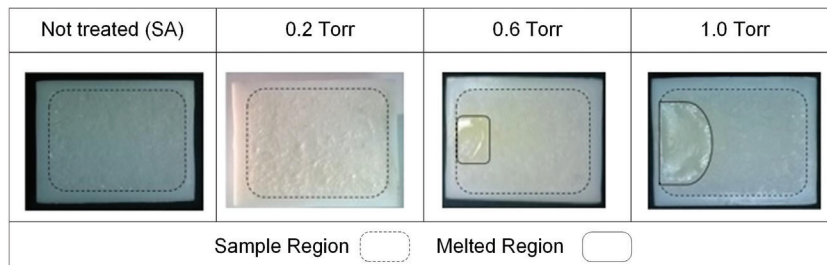
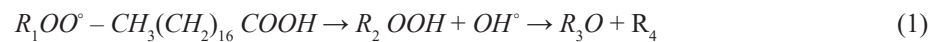


**Figure 2:** Visual aspect of the specimens, showing the sample region (dotted line) and melted region (solid line).

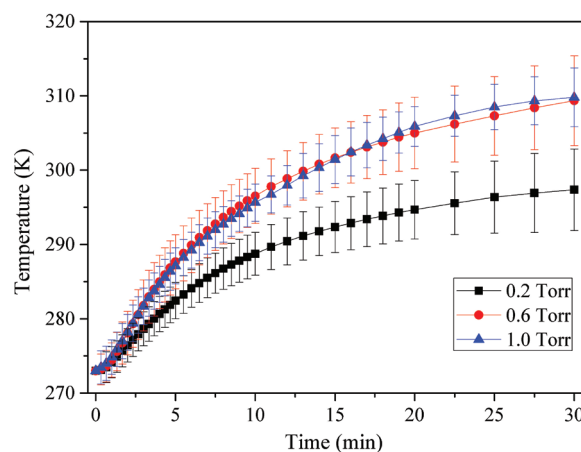


**Figure 3:** Evolution of specimen's temperature as a function of treatment time.

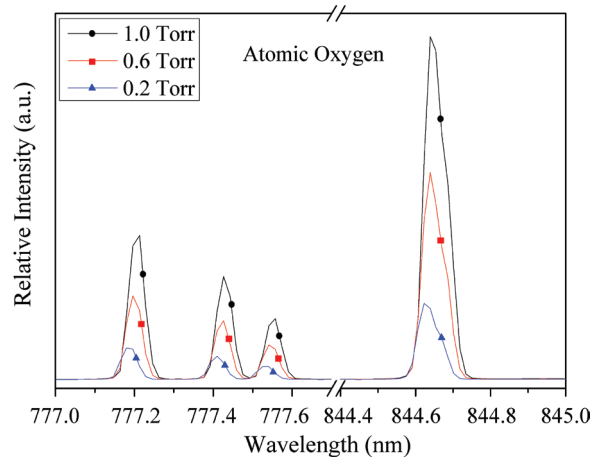


**Figure 4:** Optical emission spectra of the discharge at different pressures.

For higher pressures, the amount of charged species - ions and electrons - is also higher, increasing the heating of the specimens since those charged species collide with their surfaces releasing energy in the form of heat [18]. In other hand, from 0.2 to 1.0 Torr there is an important grow in the density of oxygen active species, which reaction with organic material is independent of electrical fields.

Considering the effects of charged and electrical neutral species, the amount of energy (physical and chemical) delivered at the surface can cause the melting of the samples (Figure 3) and the formation of volatile compounds, with subsequent degradation of stearic acid. Higher molecular and atomic oxygen concentrations, together with higher densities of charged species available with the increasing treatment pressures, accelerate the degradation process of stearic acid. As presented by BERNARDELLI *et al.* [18], there is a synergic effect of charged and neutral species. Whereas charged species can hit the stearic acid with higher energy than the neutrals, the superior number of chemically reactive (but electrically neutral) oxygen species collaborates to etch the studied material.

This effect can be observed in Figure 2, where a higher amount of liquid phase is formed for the most elevated working pressure. This also agrees with the temperature increase for higher pressures, as shown in Figure 3.

Figure 5 shows the results regarding mass loss as a function of treatment pressure. Mass loss was observed for all treatment conditions, and the higher mass variation occurred for specimens treated at 0.2 and 0.6 Torr. Mass loss for samples treated at 0.6 Torr was higher (although very close) to those treated at 0.2 Torr, where the specimens were not melting.

The presence of the liquid phase and its amount is crucial for the mass loss phenomenon. While the material remains in the solid phase, reactions that lead to chain breakage and consequent formation of volatile compounds are favored and increase the etching rate. In opposition, the active oxygen species can diffuse in the liquid phase and react [27], leading to the ramification of carbon chains [12, 24, 28]. In this case, organic compounds of higher molecular weight will be formed, and their removal becomes more difficult. As the pressure increases, the concentrations of reacting species (charged or not) increases, changing the behavior of the treated material. Under the studied conditions, the reaction seems to have reached a limit when increasing the pressure to 0.6 Torr. At this pressure, partial sample melting was observed in some experiments but not for all repetitions. Even with the etching of the solid portion, the higher volume of the liquid phase at 1.0 Torr favors the oxygen absorption on the material, leading to lower mass loss.

Mass spectroscopy results regarding the volatile products formed as a result of stearic acid degradation are shown in Figure 6. The partial pressure of the main reaction products was followed and plotted during the treatment. In these results it is possible to evaluate the relative amount of volatile products formed when the stearic acid is submitted to an Ar + 10% O<sub>2</sub> plasma.

From the mass spectroscopy data (Figure 6), it can be observed that the following volatile products are formed as a result of the stearic acid degradation: m/z 28 (CO), 44 (CO<sub>2</sub>), 2 (H<sub>2</sub>), 18 (H<sub>2</sub>O), 14 (C), 34 (C<sub>2</sub>H<sub>6</sub>) and 17 (CH<sub>3</sub>). H, H<sub>2</sub>O, CO, and CO<sub>2</sub> are the main compounds, while the amount of C, C<sub>2</sub>H<sub>6</sub>, and CH<sub>3</sub> is lower. The formation of such volatile products follows a similar pattern for all treatment conditions: a high formation rate at the beginning of treatment, stabilizing until the end of the treatment (30 minutes), as seen in Figure 6.

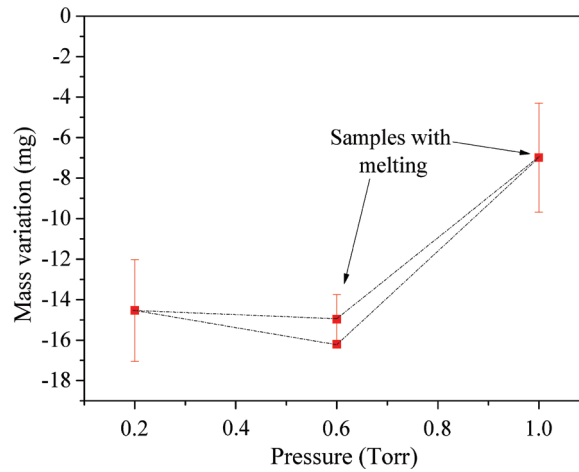


Figure 5: Mass loss as a function of treatment pressure.

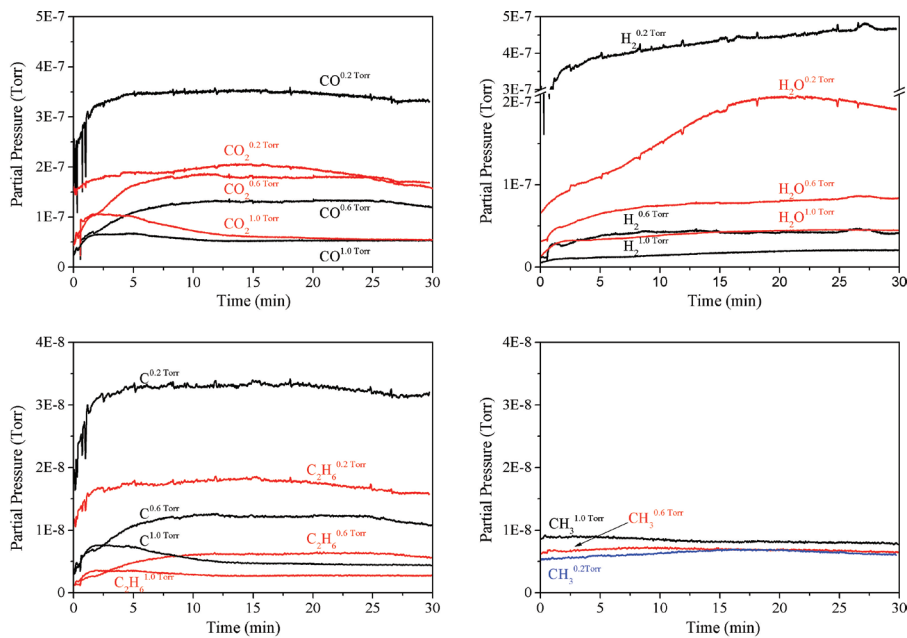


Figure 6: Main by-products from the plasma etching of stearic acid obtained by mass spectrometry. Treatments were carried out at 0.2, 0.6, and 1.0 Torr.

The volatile products  $C_2H_6$ , C, and  $CH_3$  are generated by the fragmentation of stearic acid into shorter chains through oxidative processes [20, 25, 29] or by etching caused by charged species (ions and electrons) [14, 18].

One possible contribution to the formation of the species  $C_2H_6$ , C e  $CH_3$  is the fragmentation of alkanes of larger chains during the plasma treatment or by ionization in the mass spectrometer.  $H_2O$  is generated by hydrogen atoms released from the carbon chain to form OH groups, which then react to other hydrogen atoms forming  $H_2O$  [29–32]. Hydrogen atoms are generated by the fragmentation of  $H_2O$  during the plasma treatment or by the degradation of stearic acid caused by charged particles (ions and electrons) [14, 17, 18].

$CO$  and  $CO_2$  can be formed from two sources: oxidized products from stearic acid cracked into  $CO$  and  $CO_2$ . These reactions may occur both at the surface and the bulk of the material [20, 24, 25]. Also, they can be formed within the gaseous phase, where carbon chains resulting from stearic acid degradation could be oxidized. Regarding  $CO_2$ , it can also be generated due to  $CO$  cracking under plasma or in the mass spectrometer.

The  $CO/CO_2$  ratio is greater than 1 for treatments at 0.2 Torr and lower than 1 for pressures of 0.6 and 1.0 Torr. The higher amount of  $CO_2$  for pressures of 0.6 and 1.0 Torr must be related to the liquid phase formation

(Figure 2), which occurs because of the more intense oxidation of the stearic acid. When the treatment is done at 0.2 Torr, a lower amount of CO<sub>2</sub> is observed, and a fraction of it may be cracked, producing CO. As suggested by BIANCHI *et al.* [33], CO can be also produced by fragmentation of CO<sub>2</sub> in plasma environment, increasing the CO/CO<sub>2</sub> ratio.

The FTIR spectra are shown in Figures 7 and 8. The formation of ester groups was observed for partially melted specimens during the plasma treatment. The appearance of these ester groups is related to the broadening and increasing intensity of the peaks located between 1750 and 1700 cm<sup>-1</sup> [34]. Both broadening and peak intensity increased for increasing treatment pressures.

The formation of the ester group was possibly due to dimerization processes, where two stearic acid chains bond to each other through the acidic function. This phenomenon is triggered by the reaction with the plasma. Similar results were observed by Teixeira, *et al.* [35] in their work about stearic acid, oleanolic acid, and mixtures of both. They observed the presence of in-phase and out-of-phase modes of C=O dimers in the crystalline structure of pure stearic acid at 1684 and 1708 cm<sup>-1</sup> bands.

In FARIAS *et al.* [13] stearic acid was treated in similar conditions. When the samples were treated without a cooling system, the peak intensity at 1700 cm<sup>-1</sup> increased compared to those treated with the cooling system and non-treated stearic acid. This behavior agrees with the changes associated with the visual aspect of the specimens since melted regions could be observed. They concluded that the band broadening at 1700 cm<sup>-1</sup> is related to those melted regions, indicating that the dimerization process occurred with the increase in pressure and the liquid phase formation.

In the region from 3200 to 2700 cm<sup>-1</sup>, the baseline of the spectrum was raised for higher treatment pressures. This region has a broad and intense peak characteristic of the formation of alcohol OH group [35]. No

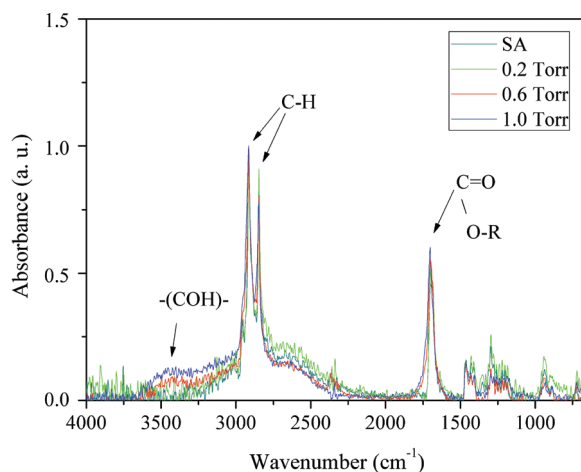


**Figure 7:** FTIR spectra of the specimens comparing untreated material and samples treated at different pressures.

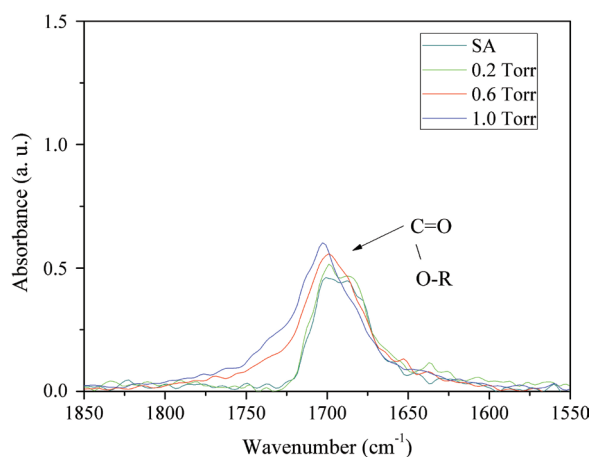


**Figure 8:** Region of the FTIR spectrum corresponding to the formation of esters.

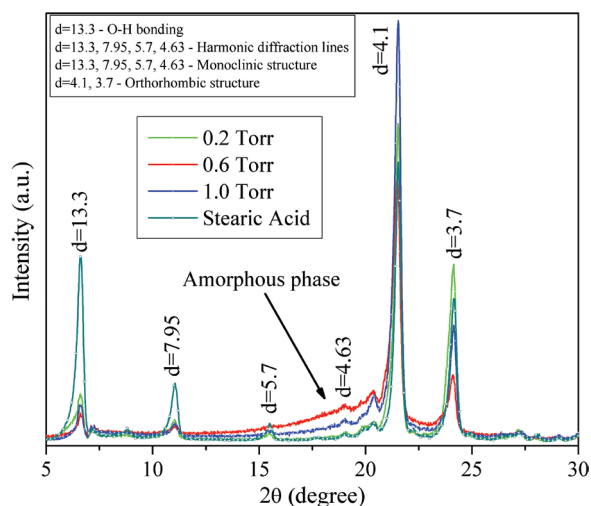


**Figure 9:** X-ray diffractograms comparing untreated material and samples treated at different pressures.

significant changes were observed for the remaining spectrum regions, indicating that the concentration of other possible functional groups could be formed below the detection limits of the technique.

The comparison between FTIR and mass loss data shows that the formation of oxidized compounds was higher (Figures 7 and 8), and the mass loss (Figure 5) was lower for specimens treated at 1.0 Torr pressure. This result shows that the etching process was predominant despite the functionalization process having occurred.

The X-ray diffractograms of the stearic acid specimens as a function of the treatment pressure are shown in Figure 9. The diffraction angles correspondent to interlamellar spacing equal to 13.3, 7.95, and 5.7 Å follow the 1/3, 1/5, and 1/7 relationship, respectively, and refer to a series of diffraction harmonic lines, representing a family of characteristic planes [35], evidencing the presence of a monoclinic structure. The peak with  $d = 13.3$  Å refers to O-H bonds in carboxyl or alcohol groups [35, 36]. Such peaks of higher interlamellar spacing correspond to the arrangement and thickness of the molecular layers of the stearic acid. The thickness of the layers is related to the size and inclination of the carbon chains [35, 36].

Peaks of 4.1 and 3.7 Å (Figure 9) are associated with the orthorhombic structure of stearic acid. According to the works of ENSIKAT *et al.* [36] and TEIXEIRA *et al.* [35] such peaks with small interplanar spacing ( $h k 0$ ) appear at high diffraction angles and are related to the lateral packing of hydrocarbon chains. It was observed that the lateral packing of hydrocarbon chains did not change as a function of treatment pressure.

The low intensity of peaks of 7.95 and 5.7 Å for treated specimens is characteristic of the lower long-range order at a given direction [35]. The same behavior is observed at the 13.3 peaks. This peak also corresponds to O-H bonding. At the moment is not possible to separate the influence of this effect and the long-range order. The reduction in peak intensity is observed for samples treated at 0.6 and 1.0 Torr pressures. This decrease in peak intensity shows that higher pressures favor breaking bonds between carboxyl groups.

BERNARDELLI *et al.* [18] showed that, in post-discharge mode, the carboxyl group is not etched when only chemically active species, excited or not, are present. However, the authors also showed that the acidic function is etched when chemically active species coexist with charged species (ions and electrons). Hence, the breaking of bonds of carboxyl groups must be associated with the bombardment by ions and electrons.

The rise of the baseline on the diffractograms (Figure 9) shows that the formation of an amorphous phase was higher for the specimens treated at 0.6 Torr. It is unexpected when considering the more significant amount of liquid phase on the treatments at 1.0 Torr. However, it can be explained as a result of a more intense modification of the smallest liquid phase volume at 0.6 Torr. As oxygen-active species can diffuse through the liquid phase [19], in 1.0 Torr experiments, the relation between oxygen/liquid material leads to a more diluted effect of the modification. On the other hand, at 0.6 Torr, the small volume of the fused material is strongly modified, resulting in higher amorphization.

#### 4. CONCLUSIONS

Stearic acid was degraded when submitted to an Ar-O<sub>2</sub> plasma at the studied pressures. The higher the pressure, the higher the liquid phase formation and reaction kinetics, resulting in higher functionalization and lower

etching, as can be verified by the reduction in the mass loss results. The presence of liquid phase results in the dimerization and amorphization of the structure. The dimerization phenomena lead to ester production because of the reaction of plasma active species with stearic acid. The main products formed due to stearic acid degradation are CO, CO<sub>2</sub>, H<sub>2</sub>, and H<sub>2</sub>O, with the highest intensities for the condition of 0.2 Torr, precisely the one with the highest mass loss. Therefore, the presence of a liquid phase is undesirable to the plasma cleaning process and needs to be avoided through the macroscopic parameters of the discharge.

## 5. ACKNOWLEDGMENTS

The authors are thankful to Brazilian Agencies CNPq and CAPES for financial support and Fundação Araucária for the fellowship granted to the student who participated in this research project.

## 6. BIBLIOGRAPHY

- [1] DALCIN, R.L., ROCHA, A.S., CASTRO, V.V., *et al.*, “Microstructure and wear properties of a low carbon bainitic steel on plasma nitriding at different N<sub>2</sub>-H<sub>2</sub> gas mixtures”, *Materials Research*, v. 25, pp. e20210447, 2022. doi: <http://dx.doi.org/10.1590/1980-5373-mr-2021-0447>
- [2] MORETTI, M.L., RECCO, A.A.C., “Duplex treatment on AISI D2 tool steel: plasma nitriding and reactive deposition of TiN and TiAlN films via magnetron sputtering”, *Matéria (Rio de Janeiro)*, v. 27, n. 3, pp. e20220111, 2022. doi: <http://dx.doi.org/10.1590/1517-7076-rmat-2022-0111>
- [3] WENISH, G.D., PRINCE, M., MANIRAJ, J., “Characterization of induction hardened and tempered AISI 1045 steel”, *Matéria (Rio de Janeiro)*, v. 27, n. 4, pp. e20220170, 2022. doi: <http://dx.doi.org/10.1590/1517-7076-rmat-2022-0170>
- [4] BEILNER, G., PEREIRA, B.L., LEPIENSKI, C.M., *et al.*, “Ti-25Nb-25Ta alloy treated by plasma electrolytic oxidation in phosphoric acid for implant applications”, *Matéria (Rio de Janeiro)*, v. 26, n. 1, pp. e12933, 2021. doi: <http://dx.doi.org/10.1590/s1517-707620210001.1233>
- [5] BELKIND, A., KROMMENHOESK, S., LI, H., *et al.*, “Removal of oil from metals by plasma techniques”, *Surface and Coatings Technology*, v. 68–69, pp. 804–808, 1994. doi: [http://dx.doi.org/10.1016/0257-8972\(94\)90257-7](http://dx.doi.org/10.1016/0257-8972(94)90257-7)
- [6] KORZEC, D., RAPP, J., THEIRISH, D., *et al.*, “Cleaning of metal parts in oxygen radio frequency plasma: process study”, *Journal of Vacuum Science & Technology. A, Vacuum, Surfaces, and Films*, v. 12, n. 2, pp. 369–378, 1994. doi: <http://dx.doi.org/10.1116/1.579249>
- [7] FESSMANN, J., GRÜNWARD, H., “Plasma treatments for cleaning of metals parts”, *Surface and Coatings Technology*, v. 59, n. 1–3, pp. 290–296, 1993. doi: [http://dx.doi.org/10.1016/0257-8972\(93\)90099-A](http://dx.doi.org/10.1016/0257-8972(93)90099-A)
- [8] STEFFEN, H., SCHWARZ, J., KERSTEN, H., *et al.*, “Process control of RF plasma assisted surface cleaning”, *Thin Solid Films*, v. 283, n. 1-2, pp. 158–164, 1996. doi: [http://dx.doi.org/10.1016/0040-6090\(96\)08535-5](http://dx.doi.org/10.1016/0040-6090(96)08535-5)
- [9] KEGEL, B., SCHMID, H., “Low-pressure plasma cleaning of metallic surfaces on industrial scale”, *Surface and Coatings Technology*, v. 112, n. 1–3, pp. 63–66, 1999. doi: [http://dx.doi.org/10.1016/S0257-8972\(98\)00766-X](http://dx.doi.org/10.1016/S0257-8972(98)00766-X)
- [10] PETASH, W., KEGEL, B., SCHMID, H., *et al.*, “Low pressure cleaning: a process for precision cleaning applications”, *Surface and Coatings Technology*, v. 97, n. 1–3, pp. 176–181, 1997. doi: [http://dx.doi.org/10.1016/S0257-8972\(97\)00143-6](http://dx.doi.org/10.1016/S0257-8972(97)00143-6)
- [11] LAZZARI, L.K., NEVES, R.M., VANZETTO, A.B., *et al.*, “Thermal degradation kinetics and lifetime prediction of cellulose biomass cryogels reinforced by its pyrolysis waste”, *Materials Research*, v. 25, pp. e20210455, 2022. doi: <http://dx.doi.org/10.1590/1980-5373-mr-2021-0455>
- [12] MAFRA, M., BELMONTE, T., PONCIN-EPAILLARD, F., *et al.*, “Role of temperature on the interaction mechanisms between argon-oxygen post-discharge and hexatriacontane”, *Plasma Chemistry and Plasma Processing*, v. 28, n. 4, pp. 495–509, 2008. doi: <http://dx.doi.org/10.1007/s11090-008-9140-4>
- [13] FARIAS, C.E., BIANCHI, J.C., DE OLIVEIRA, P.R., *et al.*, “Evaluation of sample temperature and applied power on degradation of stearic acid in inductively coupled radio frequency plasma”, *Materials Research*, v. 17, n. 5, pp. 1251–1259, 2014. doi: <http://dx.doi.org/10.1590/1516-1439.270714>
- [14] BERNARDELLI, E.A., SOUZA, T., MAFRA, M., *et al.*, “Modification of stearic acid in Ar and Ar-O<sub>2</sub> pulsed dc discharge”, *Materials Research*, v. 14, n. 4, pp. 519–523, 2011. doi: <http://dx.doi.org/10.1590/S1516-14392011005000068>



- [15] CONRADS, H., SCHMIDT, M., “Plasma generation and plasma sources”, *Plasma Sources Science & Technology*, v. 9, n. 4, pp. 441–454, 2000. doi: <http://dx.doi.org/10.1088/0963-0252/9/4/301>
- [16] MURILLO, R., PONCIN-EPAILLARD, F., SEGUI, Y., “Plasma etching of organic material: combined effects of charged and neutral species”, *The European Physical Journal Applied Physics*, v. 9, n. 3, pp. 299–305, 2007. doi: <http://dx.doi.org/10.1051/epjap:2007031>
- [17] BERNARDELLI, E.A., SOUZA, T., MALISKA, A.M., *et al.*, “Plasma etching of stearic acid in Ar and Ar-O<sub>2</sub> DC discharges”, *Materials Science Forum*, v. 660–661, pp. 599–604, 2010. doi: <http://dx.doi.org/10.4028/www.scientific.net/MSF.660-661.599>
- [18] BERNARDELLI, E.A., MAFRA, M., MALISKA, A.M., *et al.*, “Influence of neutral and charged species on the plasma degradation of stearic acid”, *Materials Research*, v. 16, n. 2, pp. 385–391, 2013. doi: <http://dx.doi.org/10.1590/S1516-14392013005000008>
- [19] BERNARDELLI, E.A., BELMONTE, T., DUDAY, D., *et al.*, “Interaction mechanisms between Ar-O<sub>2</sub> post discharge and stearic acid II: behavior of thick films”, *Plasma Chemistry and Plasma Processing*, v. 31, n. 1, pp. 205–215, 2011. doi: <http://dx.doi.org/10.1007/s11090-010-9264-1>
- [20] BELMONTE, T., BERNARDELLI, E.A., MAFRA, M., *et al.*, “Comparison between hexatriacontane and stearic acid behavior under late Ar-O<sub>2</sub> post discharge”, *Surface and Coatings Technology*, v. 205, n. 2, pp. S443–S446, 2011. doi: <http://dx.doi.org/10.1016/j.surfcoat.2011.03.041>
- [21] FARIAS, C.E., BERNARDELLI, E.A., BORGES, P.C., *et al.*, “Determination of surface temperature in ICP RF plasma treatments of organic materials”, *Materials Research*, v. 20, n. 5, pp. 1432–1443, 2017. doi: <http://dx.doi.org/10.1590/1980-5373-mr-2017-0238>
- [22] FARIAS, C.E., BERNARDELLI, E.A., BORGES, P.C., *et al.*, “Dependence of E-H transition in argon ICP discharges for treatment of organic molecules”, *Matéria*, v. 22, n. Suppl. 1, pp. e11920, 2017. doi: <https://doi.org/10.1590/S1517-707620170005.0256>
- [23] SCHEUER, C.J., CARDOSO, R.P., MAFRA, M., *et al.*, “Effects of the voltage and pressure on the carburizing of martensitic stainless steel in pulsed DC glow discharge”, *Materials Research*, v. 24, n. 6, pp. e20210154, 2021. doi: <http://dx.doi.org/10.1590/1980-5373-mr-2021-0154>
- [24] BERNARDELLI, E.A., BELMONTE, T., DUDAY, D., *et al.*, “Interaction mechanisms between Ar-O<sub>2</sub> post discharge and stearic acid I: behaviour of thin films”, *Plasma Chemistry and Plasma Processing*, v. 31, n. 1, pp. 189–203, 2011. doi: <http://dx.doi.org/10.1007/s11090-010-9263-2>
- [25] TAUBE, H., “Mechanisms of oxidation with oxygen”, *The Journal of General Physiology*, v. 49, n. 1, pp. 29–52, 1965. doi: <http://dx.doi.org/10.1085/jgp.49.1.29>. PMID: 5859925.
- [26] SHELDON, R.A., KOCHI, J.K., “Metal Catalysis in Peroxide Reactions. Metal-catalyzed Oxidations of Organic Compounds”, New York, USA, Academic Press, pp. 33–70, 1981. doi: <https://doi.org/10.1016/B978-0-12-639380-4.50009-9>
- [27] MAFRA, M., BELMONTE, T., MALISKA, A.M., *et al.*, “Argon-oxygen post-discharge treatment of hexatriacontane: heat transfer between gas phase and sample.”, *Key Engineering Materials*, v. 373–374, pp. 421–425, 2008. doi: <http://dx.doi.org/10.4028/www.scientific.net/KEM.373-374.421>
- [28] MAFRA, M., BELMONTE, T., PONCIN-EPAILLARD, F., *et al.*, “Treatment of hexatriacontane by Ar-O<sub>2</sub> remote plasma: formation of the active species”, *Plasma Processes and Polymers*, v. 6, n. S1, pp. S198–S203, 2009. doi: <http://dx.doi.org/10.1002/ppap.200932406>
- [29] NORMAND, F., GRANIER, A., LEPRINCE, P., *et al.*, “Polymer treatment in the flowing afterglow of an oxygen microwave discharge: active species profile concentrations and kinetics of the functionalization”, *Plasma Chemistry and Plasma Processing*, v. 15, n. 2, pp. 173–198, 1995. doi: <http://dx.doi.org/10.1007/BF01459695>
- [30] NARAYANASWAMY, K., PEPIOT, P., PITSCH, H., “A chemical mechanism for low to high temperature oxidation of n-dodecane as a component of transportation fuel surrogates”, *Combustion and Flame*, v. 161, n. 4, pp. 866–884, 2013. doi: <http://dx.doi.org/10.1016/j.combustflame.2013.10.012>
- [31] SOLOVEICHIK, S., KRAKAUER, H., “Oxidation stages of organic aliphatic compounds: a classification scheme”, *Journal of Chemical Education*, v. 43, n. 10, pp. 532–535, 1996. doi: <http://dx.doi.org/10.1021/ed043p532>
- [32] ALLEN, S., EDGE, M., RODRIGUEZ, M., *et al.*, “Aspects of the thermal oxidation, yellowing and stabilisation of ethylene vinyl acetate copolymer”, *Polymer Degradation & Stability*, v. 71, n. 1, pp. 1–14, 2000. doi: [http://dx.doi.org/10.1016/S0141-3910\(00\)00111-7](http://dx.doi.org/10.1016/S0141-3910(00)00111-7)

- [33] BIANCHI, J.C., FARIAS, C.E., BERNARDELLI, E.A., *et al.*, “Influence of applied plasma power on degradation of L-proline in an inductively coupled RF plasma reactor”, *Matéria (Rio de Janeiro)*, v. 27, n. 4, pp. e202248897, 2022. doi: <http://dx.doi.org/10.1590/1517-7076-rmat-2022-48897>
- [34] SILVERSTEIN, R.M., WEBSTER, F.X., KIEMLE, D.J., *Spectrometric identification of organic compounds*, 7 ed., New York, John Wiley & Sons, 2005.
- [35] TEIXEIRA, A.C.T., GARCIA, A.R., ILHARCO, L.M., *et al.*, “Phase behavior of oleanolic acid, pure and mixed with stearic acid: interactions and crystallinity”, *Chemistry and Physics of Lipids*, v. 163, n. 7, pp. 655–666, 2010. doi: <http://dx.doi.org/10.1016/j.chemphyslip.2010.06.001>. PubMed PMID: 20599856.
- [36] ENSIKAT, H.J., BOESE, M., MADER, W., *et al.*, “Crystallinity of plant epicuticular waxes: electron and X-ray diffraction studies”, *Chemistry and Physics of Lipids*, v. 144, n. 1, pp. 45–59, 2006. doi: <http://dx.doi.org/10.1016/j.chemphyslip.2006.06.016>. PubMed PMID: 16879815.